Effects of Outer Mouth Mutations on *hERG* Channel Function: A Comparison with Similar Mutations in the *Shaker* Channel

Jing-Song Fan,[#] Min Jiang,[*] Wen Dun,[*] Thomas V. McDonald,[§] and Gea-Ny Tseng[*]

[*]Department of Pharmacology, Columbia University, New York, New York 10032; [#]Department of Physiology and Biophysics, University of Texas Medical Branch, Galveston, Texas 77555-0641; and [§]Division of Cardiology, Albert Einstein College of Medicine, Bronx, New York 10461 USA

ABSTRACT The fast-inactivation process in the *hERG* channel can be affected by mutations in the pore or S6 domain, similar to the C-type inactivation in the *Shaker* channel. However, differences in the kinetics and voltage dependence of inactivation between these two channels suggest that different structural determinants may be involved. To explore this possibility, we mutated a serine in the outer mouth region of *hERG* (S631) to residues of different physicochemical properties and compared the resulting changes in the channel's inactivation process with those resulting from mutations of an equivalent position in the *Shaker* channel (T449). The most dramatic differences are seen when this position is occupied by a charged residue: S631K and S631E disrupted C-type inactivation in *hERG*, whereas T449K and T449E facilitate C-type inactivation in *Shaker*. S631K and S631E also disrupted the K selectivity of *hERG* pore, a change not seen in T449K or T449E of *Shaker*. To further study why there are such differences, we replaced S631 with cysteine. This allowed us to manipulate the properties of thiol groups at position 631 and correlate side-chain properties here with changes in channel function. S631C behaved like the wild-type channel when the thiol groups were in the reduced state. Oxidizing thiol groups with H_2O_2 or modifying them with MTSET or MTSES disrupted C-type inactivation and K selectivity, similar to the phenotype of S631K and S631E. The same thiol-modifying maneuvers did not affect the wild-type channel function. Our results suggest differences in the outer mouth structure between *hERG* and *Shaker*, and we propose a "molecular spring" hypothesis to explain these differences.

INTRODUCTION

The rapid component of delayed rectifier channel (I_{Kr}) in cardiac myocytes plays an important role in maintaining the electrical stability of the heart (Roden et al., 1996). Under physiological conditions, current through the I_{Kr} channel displays an inward rectification: current amplitude is reduced in the plateau voltage range but increases rapidly when the membrane is repolarized (Zhou et al., 1998). This inward rectification economizes the amount of inward current required to maintain the plateau phase of cardiac action potential, yet provides sufficient outward current in the negative voltage range to ensure proper repolarization (Hancox et al., 1998).

The availability of cDNA encoding for the I_{Kr} channel (*hERG*) has greatly aided the investigation of molecular mechanism underlying the inward rectification in the I_{Kr} channel (Sanguinetti et al., 1995). It has been shown that the inward rectification of the *hERG* (and thus I_{Kr}) channel is due to a fast-inactivation process (Spector et al., 1996) that has characteristics similar to those of C-type inactivation described for the *Shaker* and related K channels (Panyi et al., 1995; Liu et al., 1996; Hoshi et al., 1991). Studies on the *Shaker* channel have suggested that C-type inactivation involves concerted conformational changes of channel subunits, leading to an occlusion of K ion flux through the pore (Panyi et al., 1995; Ogielska et al., 1995). This is due to either a constriction of the external entrance to the pore (Yellen et al., 1994; Liu et al., 1996) or an alteration of the selectivity filter, so that K ion flux becomes impossible under physiological ionic conditions (Starkus et al., 1997).

Elevating $[K]_o$ or blocking the outer mouth by a submaximum concentration of tetraethylammonium (TEA) slows the rate of C-type inactivation in *Shaker* as well as the fast inactivation in *hERG* (Choi et al., 1991; Smith et al., 1996; Baukrowitz and Yellen, 1995; Wang et al., 1996). More importantly, mutations made in the P-loop sequence or in the S6 domain can affect both inactivation processes, pointing to a common inactivation mechanism involving the outer mouth region (Ficker et al., 1998; Zou et al., 1998; Schonherr and Heinemann, 1996; Smith et al., 1996; Herzberg et al., 1998; Hoshi et al., 1991). Despite these similarities, there are important differences in the kinetics and voltage dependence of C-type inactivation between these two channels (Rasmusson et al., 1998). In *hERG*, the onset and reversal of C-type inactivation precede or occur simultaneously with channel activation and deactivation, respectively. On the other hand, in *Shaker* the onset or reversal of C-type inactivation is much slower and occurs only after the activation or deactivation process has largely reached a steady state. C-type inactivation in *hERG* displays a strong voltage dependence. This is in sharp contrast to the lack of intrinsic voltage dependence in *Shaker*'s C-type inactivation process.

There can be two possible explanations for these differences. First, the inactivation process in *hERG* may have its own voltage-sensing mechanism different from that mediated by the S4 domain. This voltage-sensing mechanism causes fast and voltage-dependent onset and reversal of

Received for publication 5 January 1999 and in final form 1 March 1999.

Address reprint requests to Dr. Gea-Ny Tseng, Department of Pharmacology, Columbia University, 630 West 168th Street, New York, NY 10032. Tel.: 212-305-4166; Fax: 212-305-8780; E-mail: gt10@columbia.edu.

0006-3495/99/06/3128/13 $2.00

inactivation in *hERG*, independent of channel activation and deactivation associated with S4 movements (Larsson et al., 1996). The *Shaker* channel lacks such an independent voltage-sensing mechanism. Its C-type inactivation is coupled to the activation and deactivation processes initiated by S4 movements. The second possibility is that S4 is the only voltage sensor for gating in both channels, but the coupling between S4 movements and conformational changes in the outer mouth region is much more efficient in *hERG* than in *Shaker*. Therefore, in *hERG* the fast conformational changes in the outer mouth region directly reflect the time course and voltage dependence of S4 movements. On the other hand, in *Shaker* the slow conformational changes in the outer mouth region lag behind S4 movements.

One way to study this issue is to compare the effects of equivalent mutations on C-type inactivation between *hERG* and *Shaker*. Differences in the effects may reveal altered structural elements involved in these inactivation processes. An important residue for C-type inactivation in the *Shaker* channel is threonine at position 449 (T449) (Ogielska et al., 1995; Lopez-Barneo et al., 1993; Hoshi et al., 1991). This is also one of the most extensively studied residues in the *Shaker* channel. This position is at the carboxy end of the P-loop sequence. Physically, it is located at the edge of the outer mouth of the pore (Fig. 1) (Doyle et al., 1998). This strategic location can explain why the physicochemical properties of side chain at this position can affect the rate and degree of C-type inactivation in the *Shaker* channel (Ogielska et al., 1995; Lopez-Barneo et al., 1993). Putting a bulky hydrophobic residue (T449V) or an aromatic residue (T449Y) at this position hinders C-type inactivation, whereas a hydrophilic residue (T449K or T449E) can greatly facilitate C-type inactivation. A small hydrophobic residue here (T449A) can also enhance the rate of C-type inactivation. These results have led to the hypothesis that conformational changes during C-type inactivation in the *Shaker* channel involve a translocation of residue at position 449, exposing it to the aqueous phase (Yellen et al., 1994; Liu et al., 1996). Therefore a hydrophilic side chain here stabilizes the channel in the C-type inactivated state.

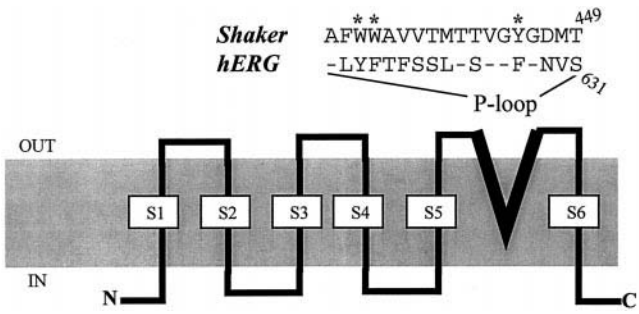

FIGURE 1 Schematic diagram of the transmembrane topology of one subunit of voltage-gated K channels. The amino (N) and carboxy (C) termini as well as the six transmembrane segments (S1 to S6) are labeled. The "P-loop" is highlighted by thick lines. The P-loop amino acid sequences of *Shaker* and *hERG* channels are aligned on top (- indicates identical amino acids). The alignment is based on the absolutely conserved "GXG" signature sequence of K channel pores. The residue at the carboxy end of the P-loop sequence is T449 (*Shaker*) or S631 (*hERG*).

The equivalent position in the *hERG* channel is 631, which is occupied by serine (S631, Fig. 1). In the present study, we mutated S631 to residues with different side-chain properties and addressed the following four questions: 1) What are the effects of these mutations on C-type inactivation of the *hERG* channel? 2) What are the effects of these mutations on other channel functions, such as ion selectivity and voltage dependence of activation? 3) Are the changes induced by these mutations similar to, or different from, those induced by equivalent mutations of T449 in the *Shaker* channel? and 4) Based on these results and the crystal structure of a K channel pore (Doyle et al., 1998), can we provide some explanation for why the C-type inactivation process differs between *hERG* and *Shaker*?

MATERIALS AND METHODS

Site-directed mutagenesis and cRNA in vitro transcription

hERG WT (in pGH19, a gift from Dr. G. Robertson; Trudeau et al., 1995) was subcloned into a vector, pAlter-Max, that is part of a mutagenesis kit (Altered Sites II Mammalian Mutagenesis System, Promega). Oligonucleotide-directed mutagenesis reactions were carried out according to the manufacturer's instructions. Plasmid DNAs were linearized by *Xba*I for in vitro transcription. The transcription reactions were performed using a commercial kit (mMessage mMachine, Ambion, Austin, TX) and T7 RNA polymerase. Denaturing agarose gel electrophoresis was used to check the quality of cRNA product of each transcription reaction and to quantify the yield. cRNA was dissolved in RNase-free water for oocyte injection.

Oocyte preparation and injection

The oocytes of *Xenopus laevis* were isolated by partial ovariectomy. Follicular cell layers were removed mechanically after mild digestion with collagenase (type B; Boehringer Mannheim, Indianapolis, IN). Four to six hours after isolation, oocytes were injected with cRNA solutions, using a Drummond digital microdispenser. The volume injected was 30–50 nl per oocyte. The oocytes were incubated at 16°C in an ND 96 solution (mM: 96 NaCl, 2 KCl, 1.8 $CaCl_2$, 1 $MgCl_2$, 5 HEPES, 2.5 Na-pyruvate, pH 7.5 with NaOH), supplemented with penicillin (50 U/ml), streptomycin (50 μg/ml), gentamycin (10 μg/ml), and horse serum (4%). The oocytes were studied 2–6 days after injection.

Electrophysiological experiments

The oocytes were placed in a tissue chamber and superfused at room temperature (23–25°C) with a low Cl solution to minimize interference from endogenous Ca-activated Cl currents. The solution had the following composition (mM): 96 NaOH, 2 KOH, 1 $MgSO_4$, 1.8 $CaCl_2$, 5 HEPES, 2.5 Na-pyruvate (pH 7.5 with methanesulfonic acid). The flow rate was maintained at ~10 ml/min, allowing a total exchange of the bath solution in 15–30 s after switching the valve that controlled the solution flowing into the bath. Membrane currents were studied using the two-microelectrode voltage clamp technique, with an Oocyte Clamp amplifier (model OC-725B; Warner Instrument Corp, MA). Both the voltage-recording and the current-passing electrodes were made of agarose-cushion pipettes of low tip resistance (0.1–0.2 MΩ) to improve the quality of voltage clamp (Schreibmayer et al., 1994).

Solutions and chemicals

The Na-free bath solution was made by replacing NaOH with equimolar *N*-methyl-D-glucamine (NMG). Dithiothreitol (DTT) was dissolved in distilled water at 0.5 M, aliquoted, and stored at −20°C. Each aliquot was used for one experiment by diluting with bath solution to reach a final concentration of 5 mM right before the experiment. H_2O_2 was added to the bath solution right before experiment to reach a final concentration of 0.1%. MTSET and MTSES (Toronto Research Company) were aliquoted and stored at −20°C. Each vial contained enough powder to make 100 ml of 2.5 mM solution. For each experiment, after the control data were recorded, a vial of MTSET or MTSES was added to 100 ml bath solution and used to superfuse the oocyte for ~10 min. This was followed by a wash of 10 min before data were collected as "after MTS treatment."

Data acquisition

The generation of voltage clamp protocols and data acquisition were controlled by an IBM/AT-compatible computer with Clampex of pClamp via a 12-bit D/A and A/D converter (TL-1 DMA Interface; Axon Instruments). Currents were low-pass filtered with an 8-pole Bessel filter (Frequency Devices, Haverhill, MA) at 2 kHz, digitized on-line, and stored on diskettes for off-line analysis. The sampling interval for whole-cell currents ranged from 0.1 to 1 ms.

Voltage clamp protocols and data analysis

Fig. 2 illustrates the voltage clamp protocols we used to characterize the current-voltage relationship and voltage dependence of activation of the wild-type *hERG* channel. Similar voltage clamp protocols and methods of data analysis were applied to mutant channels, with modifications noted in figure legends. In all of our voltage clamp protocols, there was a 20-ms prepulse from the holding voltage of −80 mV to −100 mV. The resulting current step was used for linear leak subtraction during data analysis. Data analysis was mainly carried out using Clampfit (version 6.1). PeakFit (Jandel Scientific, Corte Madera, CA) was used to fit the activation curves. When appropriate, data are presented as means and standard errors. Statistical analysis of unpaired *t*-test was performed using SigmaStat (Jandel Scientific Software, San Rafael, CA). Statistical significance is determined at a p value of 0.01.

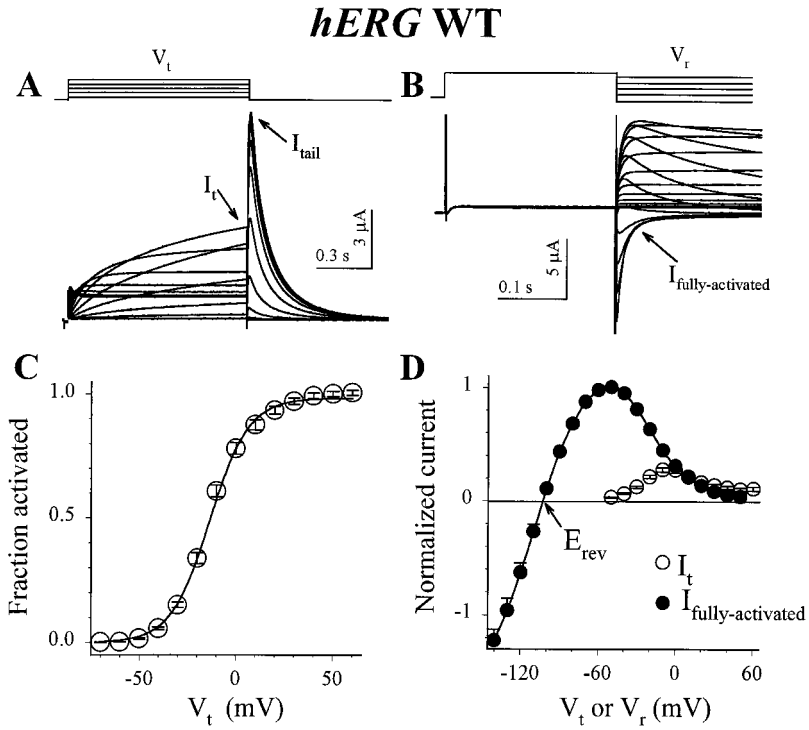

FIGURE 2 Current-voltage relationship and voltage dependence of activation of the *hERG* wild-type (WT) channel. (*A* and *B*) Original current traces recorded using the voltage clamp protocols shown on top. In *A*, the membrane voltage was stepped from a holding voltage (V_h) of −80 mV to −100 mV for 20 ms and then to test voltages (V_t) ranging from −70 to +60 mV in 10-mV increments for 1 s once every 15 s. Shown below are current traces during depolarization pulses (I_t) and the following tail currents (I_{tail}). In *B*, the membrane was depolarized from V_h −80 mV to +60 mV for 300 ms to fully activate the channels. This was followed by repolarization steps to V_r ranging from +50 to −140 mV in 10-mV increments. Plateau or peak currents recorded during the repolarization steps are defined as fully activated currents ($I_{fully\ activated}$). (*C*) Isochronal (1 s) activation curves constructed using the peak amplitudes of tail currents as shown in *A*. I_{tail} amplitudes after test pulses to various V_t were normalized by the maximum I_{tail} after a test pulse to +60 mV to give an estimate of fraction of channels activated. The relationship between the fraction of channels activated and V_t was fit with a simple Boltzmann function:

$$\text{Fraction activated} = 1/\{1 + \exp[(V_{0.5} - V_t)/k]\}, \quad (1)$$

where $V_{0.5}$ is the half-maximum activation voltage and k is the slope factor. Data were averaged from 13 experiments. The superimposed curve was calculated using Eq. 1 and the mean parameter values $V_{0.5} = -13.4$ mV and $k = 10.0$ mV. (*D*) Current-voltage relationships of I_t and $I_{fully\ activated}$. I_t amplitudes were measured at the end of test pulses as shown in *A*. $I_{fully\ activated}$ amplitudes were measured from the plateau or peak of currents during repolarization steps as shown in *B*. Both were leak-subtracted, using currents elicited by the step from −80 to −100 mV that preceded each test pulse. For each cell, both current amplitudes recorded at different voltages were normalized by the maximum $I_{fully\ activated}$ recorded at −50 mV in that same cell. Data were averaged from five experiments. In *D*, E_{rev} refers to the zero-current voltage.

RESULTS

Fig. 2 illustrates characteristics of the wild-type (WT) *hERG* channel pertinent to the present study. This figure also serves to show the voltage clamp protocols and methods of current measurement and data analysis that will be used in the following figures. The protocol shown at the top of Fig. 2 *A* was used to measure the voltage dependence of channel activation (Fig. 2 *C*) and the current-voltage (*I-V*) relationship of test pulse current (I_t in Fig. 2 *D*). The isochronal (1 s) activation curve was constructed using the *I-V* relationship of peak tail currents (I_{tail}) (Fig. 2 *C*). It could be well described by a simple Boltzmann function with a half-maximum activation voltage ($V_{0.5}$) of -13.4 ± 0.9 mV and a slope factor (k) of 10.0 ± 0.5 mV ($n = 13$). The bell-shaped *I-V* relationship of I_t reflects the voltage-dependent channel activation in the voltage range from -50 to 0 mV (ascending limb), outweighed by the inward rectification in the more positive voltage range (descending limb). As discussed in the Introduction, the inward rectification of *hERG* WT is due to a fast-inactivation process through a mechanism similar to the C-type inactivation described for the *Shaker* and other related K channels (Smith et al., 1996; Spector et al., 1996).

The protocol shown at the top of Fig. 2 *B* was used to measure the *I-V* relationship of fully activated currents ($I_{fully\ activated}$) and the reversal potential (E_{rev}) (Fig. 2 *D*). The membrane was depolarized by a prepulse to +60 mV for 300 ms, followed by repolarization steps to +50 to -140 mV. The prepulse fully activated the channels. Channel inactivation also reached a steady state during the prepulse. During the subsequent repolarization steps, the channels rapidly redistributed among inactivated and activated states with the steady state of distribution determined by the repolarization voltage. In the voltage range negative to -30 mV, this was followed by channel deactivation and a decay of current amplitude. The plateau or peak amplitudes of currents recorded during the repolarization steps were defined as fully activated currents. In Fig. 2 *D*, the difference between I_t and $I_{fully\ activated}$ in the voltage range from -50 to 0 mV reflects the voltage dependence of channel activation.

To test how changing side chain properties at position 631 could affect the C-type inactivation process in *hERG*, we mutated S631 to a number of residues: an aromatic residue with a hydroxyl group (S631Y), hydrophobic residues with different sizes (small side chain in S631A and larger side chain in S631V), or hydrophilic residues with a positive (S631K) or a negative (S631E) charge. If the physicochemical properties of side chain at position 631 required to sustain an efficient C-type inactivation process in the *hERG* channel were the same as those for T449 in *Shaker* (see Introduction) (Ogielska et al., 1995; Lopez-Barneo et al., 1993), we expected to see a reduction in the degree of C-type inactivation in S631Y and S631V, but a stronger C-type inactivation in S631K, S631E, and S631A. We used the *I-V* relationships of test pulse currents to compare the degrees of C-type inactivation among these channels.

Effects of S631 mutations on the current-voltage relationship of test pulse current

Fig. 3 shows current traces recorded from *hERG* WT and S631 mutants elicited by test pulses ranging from -70 to +60 mV. WT shows a strong inward rectification at voltages positive to 0 mV due to the fast C-type inactivation process. In S631Y and S631A, the C-type inactivation process was retained, as evidenced by the decrease in outward currents during depolarization pulses positive to -10 mV (S631Y) or +10 mV (S631A). However, the degree C-type inactivation in these two mutants was reduced relative to that of the WT channel. In S631V and S631K, the degree of C-type inactivation was further reduced or abolished, so that current amplitudes continued to increase up to +60 mV. In

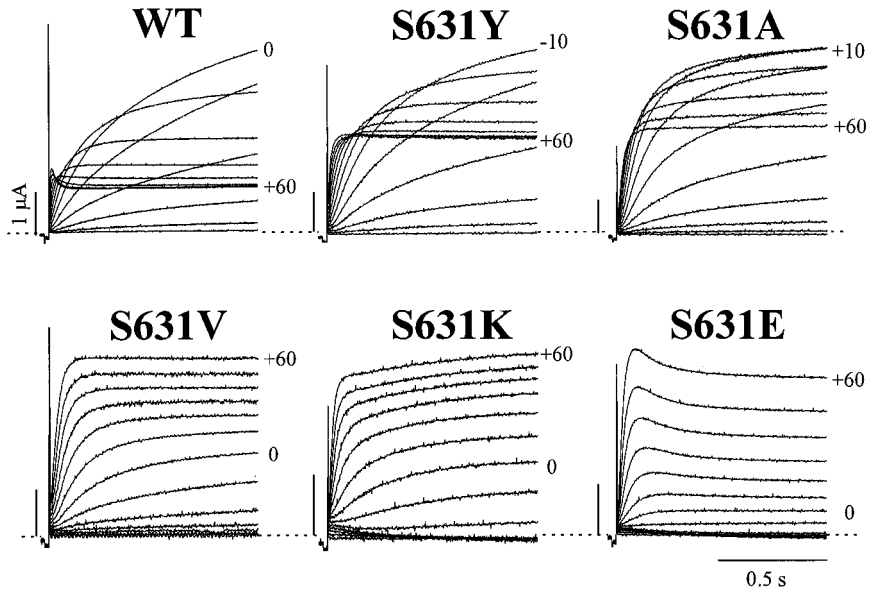

FIGURE 3 Current traces recorded from the *hERG* WT and S631 mutants, using the voltage clamp protocol described for Fig. 2 *A*. The channel type is marked on top of each panel. Numbers adjacent to current traces denote the test pulse voltages that elicited the currents.

S631E, there was a slow decay phase upon depolarization to +20 mV or more positive voltages, although the overall current amplitude showed an outward rectification. The slow decay phase of S631E suggests that this mutant has a voltage-dependent inactivation process, the rate of which is much slower than that of C-type inactivation in the WT channel.

The *I-V* relationships of test pulse currents measured from the WT and S631 mutants are summarized in Fig. 4. Again, the degree of C-type inactivation was most prominent in WT, retained (although to a lesser degree) in S631Y and S631A and apparently absent in S631V, S631K, and S631E. Therefore, only the S631V mutation had the same effect on *hERG* as that of T449V on *Shaker* (hindering C-type inactivation). The other mutations either induced different effects (S631Y sustained C-type inactivation in *hERG*, whereas T449Y hindered C-type inactivation in *Shaker*) or had opposite effects (S631A, S631K, and S631E reduced or abolished C-type inactivation in *hERG*, whereas T449A, T449K, and T449E enhanced C-type inactivation in *Shaker*).

Effects of S631 mutations on the current-voltage relationship of fully activated current and the reversal potential

Both C-type inactivation and ion selectivity are determined by residues in the outer mouth region of K channel pores. It has been suggested that these two processes are intimately related physically and functionally (Kiss and Korn, 1998; Kiss et al., 1999; Starkus et al., 1997). For example, there are data suggesting that C-type inactivated Shaker channels have altered ion selectivity (Starkus et al., 1997). Furthermore, in a chimera channel of Kv2.1/Kv1.3, K ions hinder C-type inactivation, probably by binding to the nearby selectivity filter (Kiss and Korn, 1998). We examined the possibility that S631 mutations could affect the K selectivity of the pore. In Fig. 3, the current traces recorded from S631K, S631E, and (to a lesser degree) S631V showed a time-dependent increase in the inward direction in the voltage range close to the threshold of channel activation. This is more clearly seen after the currents were leak-subtracted (Fig. 4): currents were inward during small depolarization steps (−60 to −20 mV for S631K, −60 to −10 mV for S631E, −60 to −30 mV for S631V). These observations suggest that in these mutant channels the reversal potential (E_{rev}) was shifted to positive to the threshold of activation. To confirm this, we constructed *I-V* relationships of $I_{fully\ activated}$ from the WT and mutants and measured E_{rev}. To guard against potential artifacts due to endogenous channels in the oocyte membrane, we used azimilide to partially block these channels. Azimilide blocks the WT and S631 mutant channels with an IC_{50} ranging from 3 μM (S631K) to 14 μM (S631Y) (n = 4–9 each, measured at +20 mV). It does not affect the endogenous channels in uninjected oocytes (data not shown). Therefore, in the presence of 5 μM azimilide, we expected to see a reduction of both outward and inward currents, but the reversal potential should be the same. This was confirmed for both WT and S631 mutants (data not shown). The measured reversal potentials are summarized in Table 1.

The positive shift in E_{rev} of S631V, S631K, and S631E suggests that extracellular Na ions may be able to carry charges through these mutant channels in the presence of K ions. That is, these mutant channels became less K selective than the WT channel. This was tested by replacing extracellular Na ions with a large cation, *N*-methyl-D-glucamine (NMG), that does not go through ion channels. The data are summarized in Fig. 5. Removing extracellular Na ions did not shift E_{rev} of WT, S631Y, or S631A, but caused a marked negative shift in E_{rev} of S631V, S631K, and S631E. The degrees of shift in E_{rev} correspond to permeability ratios of Na to K (P_{Na}/P_K) of 0.05, 0.09, and 0.12 for S631V, S631K, and S631E, respectively (Table 1). Therefore S631 mutations that dramatically reduced the degree or rate of C-type inactivation also interfered with the pore's

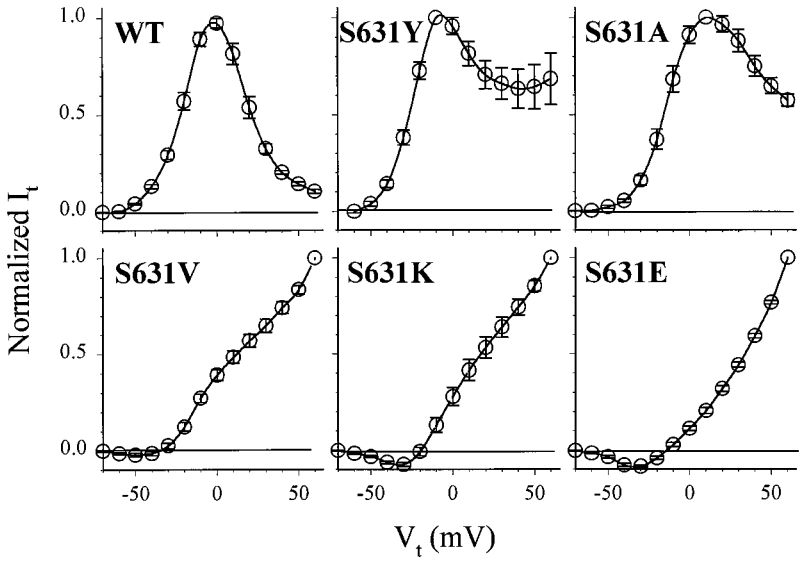

FIGURE 4 Current-voltage relationships of test pulse currents recorded from *hERG* WT and S631 mutants. The voltage clamp protocol and current measurement were the same as those described for Fig. 2, *A* and *D*. For each cell, I_t amplitudes were normalized by the maximum outward I_t measured by 0 mV (WT), −10 mV (S631Y), +10 mV (S631A), or +60 mV (S631V, S631K, and S631E). Data were averaged from 5–10 experiments for each channel.

TABLE 1 Effects of removing extracellular Na ions on the reversal potentials of the wild-type and S631 mutant channels of *hERG

	$[Na]_o$ (mM)#				
Channel	96	*n*	0	*n*	P_{Na}/P_K§
WT	−98.2 ± 0.7	12	−97.5 ± 1.9	4	—
S631Y	−98.6 ± 0.7	11	−95.0 ± 1.0	2	—
S631A	−94.5 ± 1.2	11	−94.3 ± 1.5	4	—
S631V	−59.4 ± 2.8¶	14	−91.0 ± 2.6‖	3	0.05
S631K	−24.2 ± 3.1¶	14	−66.7 ± 3.3‖	3	0.09
S631E	−12.5 ± 1.1¶	10	−61.0 ± 5.1‖	5	0.12

*Reversal potentials (E_{rev}) were determined from the *I–V* relationships of fully activated currents as shown in Fig. 2 *D*. *n*, No. of measurements.
#All solutions contained 2 mM K. In zero Na solution, equimolar *N*-methyl-D-glucamine (NMG) was added.
§The permeability ratio of Na to K (P_{Na}/P_K) was calculated based on the constant field theory (Hille, 1992), using the shift in mean E_{rev} (ΔE_{rev}) associated with Na_0 removal:

$$P_{Na}/P_K = [2*10^{(\Delta E_{rev}/58.6)} - 2]/96 \quad (3)$$

The calculation was done for S631V, S631K, and S631E. For WT, S631Y, and S631A there was no measurable Na permeability (no negative shift in E_{rev} when Na_0 was removed).
¶$p < 0.01$ versus WT.
‖$p < 0.01$ versus E_{rev} in 96 mM $[Na]_0$.

ability to discriminate against Na ions. No such effects were noted for the T449V, T449K, or T449E mutation of the Shaker channel (Ogielska et al., 1995; Lopez-Barneo et al., 1993).

As also shown in Fig. 5, removing extracellular Na ions had variable effects on the *I-V* relationships of fully activated current. In particular, in the voltage range negative to E_{rev}, removing Na_o reduced inward currents through the WT and S631Y channels, but had the opposite effect on S631A. In S631V, S631K, and S631E, removing Na_o reduced inward currents, but the degree of reduction varied among the three. These observations suggest that (other than S631Y) S631

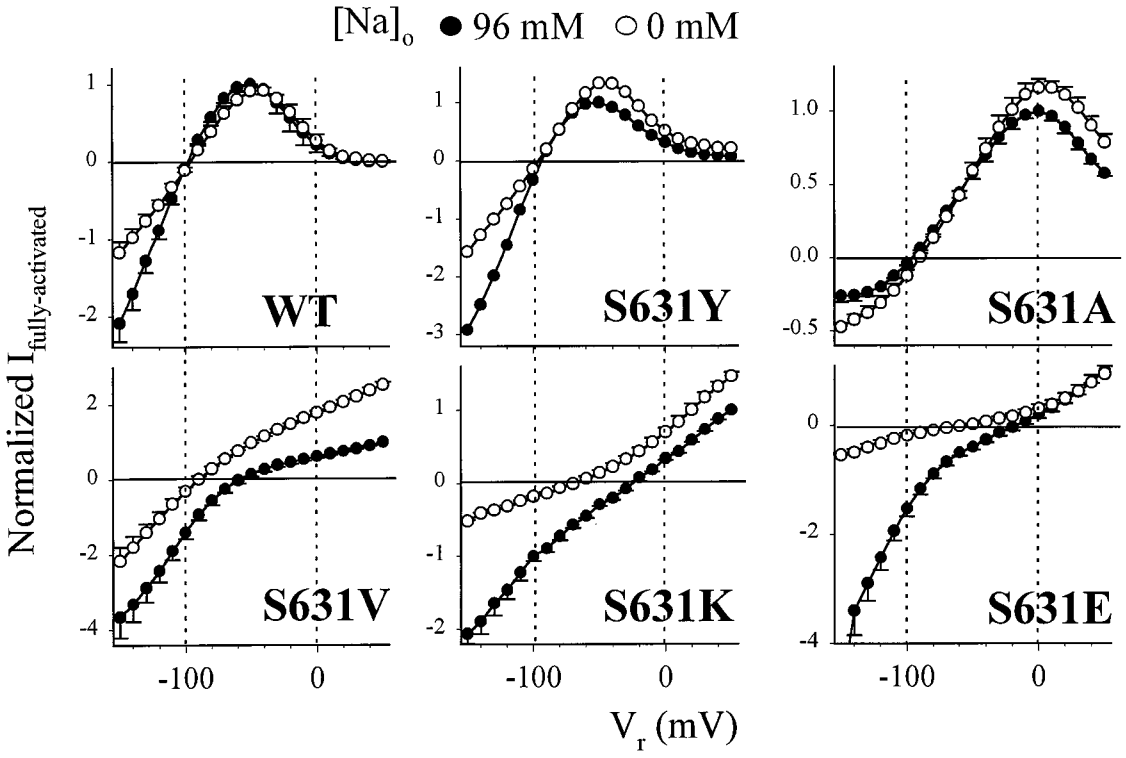

FIGURE 5 Effects of removing external Na ions on the current-voltage relationships of $I_{fully\ activated}$ and the reversal potentials of *hERG* WT and S631 mutants. The bath solution contained either 96 mM Na (●) or 0 mM Na (○, Na_o replaced by NMG). Both had 2 mM [K]. The voltage clamp protocol and current measurement were the same as those described for Fig. 2, *B* and *D*. Current amplitudes were normalized by the control current (in 96 mM $[Na]_o$) at −50 mV (WT and S631Y), 0 mV (S631A), or +50 mV (S631V, S631K and S631E). Data were averaged from three to five experiments for each channel (except S631Y, $n = 2$).

mutations could affect the modulatory effects of extracellular Na ions on ion conduction through the pores (Kiss et al., 1998; Lopez-Barneo et al., 1993).

Effects of S631 mutations on the voltage dependence of activation

Recent reports suggest that in the *Shaker* channel there are interactions between movements of residues lining the outer mouth region and movements of the voltage sensor (S4) (Loots and Isacoff, 1998; Cha and Bezanilla, 1998). The fast kinetics and strong voltage dependence of C-type inactivation in *hERG* WT point to the possibility that these two domains also interact with each other in this channel. If this is the case, mutations that alter the outer mouth structure and function (e.g., S631 mutations that disrupt C-type inactivation and K selectivity) may also affect the activation gating process. To explore this possibility, we constructed isochronal (1 s) activation curves for WT and S631 mutants. The data are summarized in Fig. 6. For S631Y and S631A, the activation curves were largely superimposable on that of the WT channel ($V_{0.5}$ values: WT -13.4 ± 1.1 mV, S631Y -17.5 ± 2.5 mV, S631A -14.5 ± 1.9 mV, $p > 0.05$ for both mutants versus WT). The activation curve of S631V was shifted in the negative direction relative to that of the WT channel ($V_{0.5} = -21.5 \pm 2.0$ mV, $p < 0.01$). For S631K and S631E, there appeared a shallow component of channel activation in the voltage range positive to -10 or -20 mV. As a result, their activation curves required an empirical double Boltzmann function for a good fit (Fig. 6). The half-maximum activation voltage of the major Boltzmann component (the one in the negative voltage range) was shifted in the hyperpolarizing direction relative to that of the WT channel ($V_{0.5}$ values: S631K -27.4 ± 1.2 and S631E -35.9 ± 1.9 mV, $p < 0.01$ for both mutants versus WT).

Therefore, S631 mutations that disrupted C-type inactivation also facilitated *hERG* channel activation in the negative voltage range. This is also suggested by the test pulse currents shown in Fig. 3: the rates of activation of S631V, S631K, and S631E appeared faster than that of the WT channel in the negative voltage range. To verify this observation, we measured and compared the time constants (τ) of activation at various test pulse voltages between WT and S631E. For the WT channel that shows a strong C-type inactivation, the τ of activation was measured by fitting a single (-20 and 0 mV) or double (-40 mV) exponential function to the envelope of peak tail currents after test pulses of different durations (Wang et al., 1997). For S631E that apparently does not C-type inactivate in the negative voltage range, τ of activation was obtained by directly fitting the current traces during depolarization with a single exponential function. At -40, -20, and 0 mV, the τ values of activation for the WT channel were 2261 ± 158 (the fast component), 717 ± 40, and 215 ± 19 ms, and those of S631E were 429 ± 38, 190 ± 37, and 54 ± 8 ms ($n = 3$–5 each). Therefore, the S631E mutation greatly accelerated channel activation in the negative voltage range.

The above data suggest that there are two types of behavior of the S631 mutants examined here. Those that

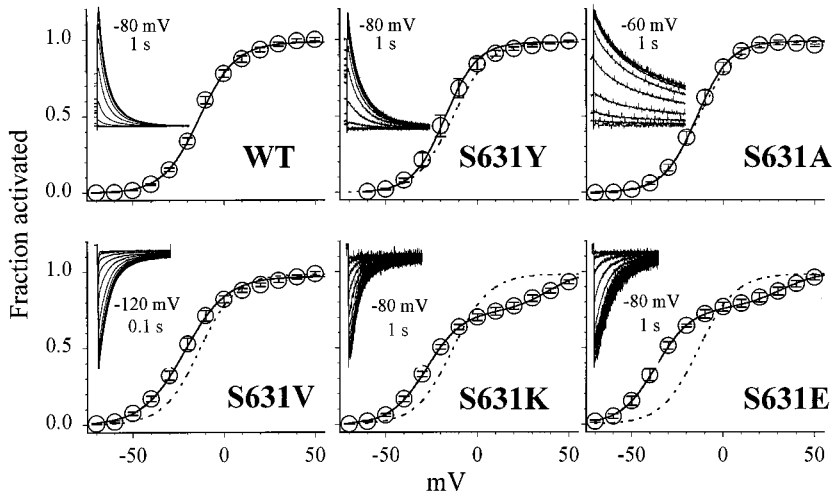

FIGURE 6 Voltage dependence of activation of *hERG* WT and S631 mutants. The voltage clamp protocol and data analysis were similar to those described for Fig. 2, *A* and *C*, except that the voltage and duration of repolarization steps at which tail currents were recorded were varied in some mutants, depending on their E_{rev}. These parameters are listed in the inset of each panel, along with representative tail current traces. Activation curves of WT, S631Y, S631A, and S631V were fit with a simple Boltzmann function (Eq. 1). Those of S631E and S631K were fit with an empirical double Boltzmann function:

$$\text{Fraction activated} = A_1/\{1 + \exp[(V_1 - V_t)/k_1]\} + (1 - A_1)/\{1 + \exp[(V_2 - V_t)/k_2]\}, \quad (2)$$

where A_1 is the fraction of the major Boltzmann component in the more negative voltage range, and V_1 and k_1 are the half-maximum activation voltage and slope factor of this component. V_2 and k_2 are the corresponding parameters of the Boltzmann component in the more positive voltage range. For each channel, data were averaged from 5–13 experiments, and the superimposed curve was calculated from Eq. 1 or 2 with mean parameter values. In panels of the mutant channels, the WT activation curve is also shown as a dotted curve for comparison.

retained the C-type inactivation process (S631Y and S631A) maintained a high K selectivity. These channels showed the same voltage dependence of activation as the WT channel. Those that disrupted C-type inactivation (S631V, S631K, and S631E) also lost K selectivity against Na and showed a negative shift in the voltage dependence of activation. To further test the linkage between side-chain properties at position 631 and channel function, we mutated S631 to cysteine (S631C). This mutation provided the advantage that the thiol groups could react with each other or with other thiol groups to form disulfide bonds (depending on the distance between them) or could be modified by thiol-specific reagents such as methanethiosulfonate (MTS) reagents. Therefore, we could manipulate the side-chain properties at position 631 and observe the resulting changes in channel function. However, because there are 21 native cysteine residues in the *hERG* WT channel (eight each in the cytoplasmic N- and C-termini, two in the extracellular S1-S2 loop, two in S5, and one in S6), we first tested whether thiol-specific reagents could alter the WT channel function.

Effects of thiol-group modification on the *hERG* WT channel

Fig. 7 summarizes the effects of a thiol-reducing agent (DTT) and an oxidizing agent (H_2O_2) on the function of *hERG* WT. There were no changes in either the *I-V* relationships of I_t and $I_{\text{fully activated}}$, or the voltage dependence of activation, although the I_t amplitude was slightly reduced after DTT treatment. Furthermore, treating oocytes with 2.5 mM MTSET or MTSES (two thiol-specific reagents) for more than 10 min had no effects on the gating function or current amplitude of *hERG* WT (data not shown). These observations indicate that either the native thiol groups of *hERG* are not reactive or accessible to these thiol-modifying reagents (e.g., cysteine residues in the intracellular or transmembrane domains), or the native thiol groups do not play important roles in channel function (e.g., the two cysteine residues on the extracellular S1-S2 linker). We then studied how modifying the thiol groups at position 631 could affect the gating function and current amplitude of the S631C mutant.

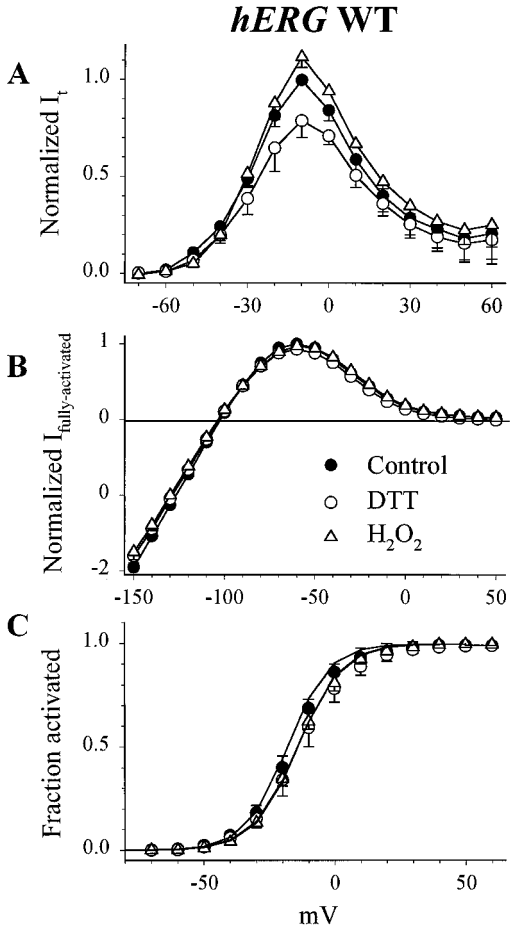

FIGURE 7 Effects of DTT or H_2O_2 on the *hERG* WT channel. Each panel shows data obtained under the control conditions (●), after 5 mM DTT treatment (○), or after 0.1% H_2O_2 treatment (△). Each data point represents the average of five experiments. (*A*) Current-voltage relationships of test pulse currents (I_t). For each cell, the amplitudes of I_t were normalized by the control I_t at −10 mV. (*B*) Current-voltage relationships of fully activated currents ($I_{\text{fully activated}}$). For each cell, the amplitudes of $I_{\text{fully activated}}$ were normalized by the control $I_{\text{fully activated}}$ measured at −60 mV. (*C*) Voltage dependence of activation. The curves superimposed on the data points were calculated from the simple Boltzmann function (Eq. 1) with mean parameter values: control, $V_{0.5} = -18.2 \pm 1.9$ mV, $k = 8.0 \pm 0.2$ mV; DTT-treated, $V_{0.5} = -14.2 \pm 3.6$ mV, $k = 8.4 \pm 0.2$ mV; H_2O_2-treated, $V_{0.5} = -14.3 \pm 1.3$ mV, $k = 8.6 \pm 0.5$ mV (one-way ANOVA: $p = 0.42$ for $V_{0.5}$ and $p = 0.43$ for k).

Effects of DTT or H_2O_2 on the *I-V* relationship and voltage dependence of activation of S631C mutant

The left panels of Fig. 8, *A* and *B*, show current traces and the *I-V* relationship of S631C recorded from an oocyte that had been treated with 5 mM DTT for 15 min. The mutant behaved like the WT channel. It displayed C-type inactivation (inward rectification in the voltage range positive to −60 mV) and a E_{rev} close to the calculated E_K. Removing external Na ions did not shift the E_{rev}, but reduced inward currents in the voltage range negative to E_{rev} similar to the behavior of the WT channel shown in Fig. 5. Treating the oocyte with 0.1% H_2O_2 led to a gradual increase in outward currents in the positive voltage range but a gradual decrease in tail currents at −80 mV, which eventually reversed the direction (becoming inward). A steady state was reached 7 min after the exposure to H_2O_2 (*right panel* of Fig. 8 *A*). At this point, the *I-V* relationship of fully activated current lost inward rectification and indicated an E_{rev} of −5 mV. Removing external Na ions shifted E_{rev} in the negative direction by 55 mV (Fig. 8 *B*, *right panel*). Subsequent washout of H_2O_2 for more than 15 min did not reverse these changes in channel properties. Similar data were obtained in 15 oocytes, although the time course of H_2O_2-induced changes in channel properties varied among oocytes (5–30 min to reach a steady state).

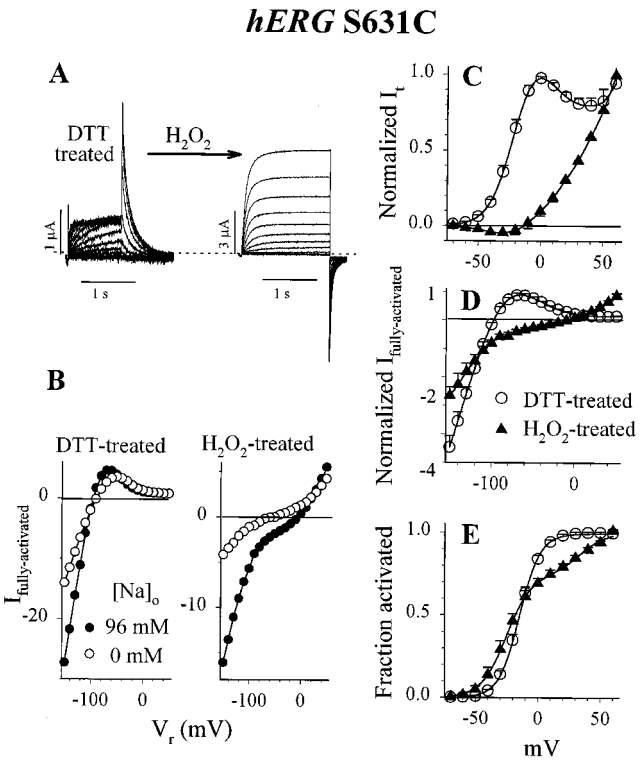

FIGURE 8 Redox state of thiol groups influences the phenotype of *hERG* S631C. (*A*) Effects of H_2O_2 (0.1%) on *hERG* S631C recorded from a DTT-treated oocyte. (*B*) Effects of removing extracellular Na ions on *hERG* S631C recorded from a DTT-treated oocyte (*left*) or from an H_2O_2-treated oocyte (*right*). The dotted line in *A* denotes the zero current level. Voltage clamp protocols and current measurement were as described for Fig. 2, except that V_r was −120 mV for current traces shown in the right part of *A*. (*C–E*) Comparison of *hERG* S631C channel properties with thiol groups in the reduced state (DTT-treated, ○) or in oxidized states (H_2O_2-treated, ▲). (*C*) The current-voltage relationships of S631C currents recorded during depolarization pulses (I_t). For each cell, I_t amplitudes were normalized by that recorded at 0 mV (DTT-treated) or at +60 mV (H_2O_2-treated). (*D*) The current-voltage relationships of fully activated *hERG* S631C currents ($I_{\text{fully activated}}$). For each cell, $I_{\text{fully activated}}$ amplitudes were normalized by that recorded at −60 mV (DTT-treated) or at +50 mV (H_2O_2-treated). (*E*) Comparison of the voltage dependencies of channel activation. The voltage clamp protocols and data analysis were the same as those described for Fig. 2. The activation curves were fit with a simple Boltzmann function (Eq. 1, DTT-treated oocytes) or an empirical double Boltzmann function (Eq. 2, H_2O_2-treated oocytes). Curves superimposed on data points were calculated using mean parameter values: DTT-treated, $V_{0.5} = -14.6 \pm 1.3$ mV, $k = 8.2 \pm 0.1$ mV; H_2O_2-treated, $A_1 = 0.72 \pm 0.04$, $V_1 = -25.9 \pm 2.5$ mV, $k_1 = 8.5 \pm 0.5$ mV, $A_2 = 0.28 \pm 0.04$, $V_2 = +32.8 \pm 2.4$ mV, $k_2 = 11.0 \pm 1.1$ mV. Each data point was averaged from nine experiments.

Fig. 8, *C–E*, summarizes the properties of S631C in oocytes treated with DTT or with H_2O_2. In DTT-treated oocytes (thiol groups in reduced state), the *I-V* relationship of $I_{\text{fully activated}}$ and the voltage dependence of activation were very similar to those of the WT channel. The *I-V* relationship of I_t showed a lesser degree of C-type inactivation (less inward rectification in the positive voltage range) than that of the WT channel. In H_2O_2-treated oocytes (thiol groups in disulfide bonds or in higher oxidized states) (Shigeru, 1989), there were a loss of C-type inactivation, a disruption of K selectivity, and changes in the activation curve (appearance of a shallow Boltzmann component in the positive voltage range, along with a hyperpolarizing shift in the major Boltzmann component in the negative voltage range). The segregation of channel properties between "WT-like" and mutant behavior by the status of thiol groups at position 631 was similar to that induced by other S631 mutations described above.

Effects of MTSET and MTSES on the *I-V* relationship and voltage dependence of activation of S631C mutant

We further examined how modifying the thiol group at 631 by MTS reagents could alter the S631C channel properties. In these experiments, oocytes had been treated with 5 mM DTT for more than 15 min before recordings. Data were obtained under such control conditions, and then after MTS treatment (10-min exposure to 2.5 mM of an MTS reagent followed by a 10-min wash period). Changes induced by the MTS reagents were not reversed after their removal, consistent with the notion that these changes resulted from a covalent modification of thiol groups. Fig. 9, *A–C*, illustrates the effects of MTSET on S631C. MTSET added a positively charged moiety to a thiol group: $\text{-CH}_2\text{-CH}_2\text{-N}^+(\text{CH}_3)_3$. This caused a switch of S631C phenotype from "WT-like" to a mutant behavior that was similar, although not identical, to that induced by H_2O_2. There were a loss of C-type inactivation, a positive shift in E_{rev} (from −100 to −20 mV, indicating a decrease in K selectivity), and changes in the activation curve (a shallow Boltzmann component in the positive voltage range and a hyperpolarizing shift of the major Boltzmann component in the negative voltage range). There appeared a slow decay phase in outward currents during depolarization steps, accompanied by a "hooked" phase in the inward tail currents at −80 mV. Similar observations were obtained in two experiments. Fig. 9, *D–F*, illustrates the effects of MTSES on S631C. MTSES added a negatively charged moiety to a thiol group: $\text{-CH}_2\text{-CH}_2\text{-SO}_3^-$. This caused a severe suppression of current amplitude. The remaining current showed a loss of C-type inactivation and a reversal of tail current direction at −80 mV. There was also a hyperpolarizing shift in the major Boltzmann component of the activation curve. Similar observations were obtained in two experiments.

Switch of S631C phenotype by repetitive depolarization pulses

S631C in oocytes that had not been treated with DTT showed a behavior intermediate between "WT-like" and mutant forms. One such example is shown in the left panel of Fig. 10. The amplitudes of test pulse currents plateaued between 0 and +20 mV, but increased again at more depolarized voltages. The tail current at −80 mV was inward

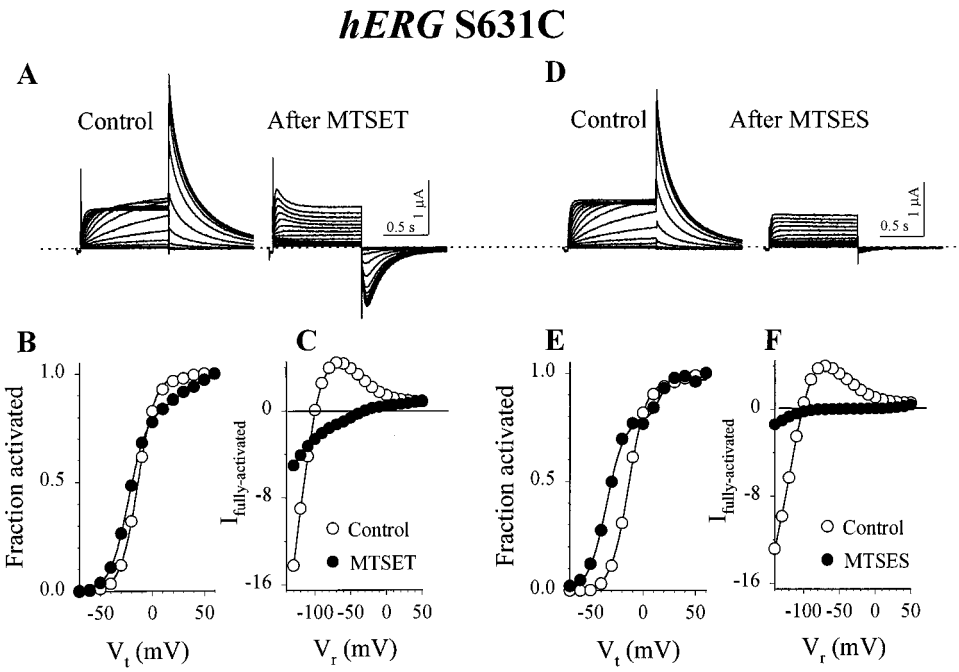

FIGURE 9 Effects of thiol-specific methanethiosulfonate reagents on *hERG* S631C. (*A*) Current traces recorded from the same oocyte before and after MTSET treatment (2.5 mM for 10 min and then wash for 10 min). The oocyte had been treated with DTT 5 mM before recording. (*B*) Effects of MTSET on the voltage dependence of activation. (*C*) Effects of MTSET on the current-voltage relationship of fully activated current. Data were from the same experiment. Voltage clamp protocols and data analysis were the same as those described for Fig. 2. In *B*, curves superimposed on data points were calculated from Eq. 1 (control, $V_{0.5} = -13.8$ mV, $k = 8.3$ mV) or Eq. 2 (after MTSET, $A_1 = 0.83$, $V_1 = -23.1$ mV, $k_1 = 8.9$ mV, $A_2 = 0.17$, $V_2 = +29.2$ mV, and $k_2 = 12.2$ mV). In *C*, E_{rev} was -100 mV under the control conditions but -20 mV after MTSET. (*D–F*) Effects of MTSES on *hERG* S631C. The format of these panels is the same as that described for *A–C*. In *E*, curves superimposed on data points were calculated from Eq. 1 (control, $V_{0.5} = -13.8$ mV, $k = 8.3$ mV) or Eq. 2 (after MTSES, $A_1 = 0.79$, $V_1 = -34.9$ mV, $k_1 = 8.4$ mV, $A_2 = 0.21$, $V_2 = +16.7$ mV, and $k_2 = 5.4$ mV).

after a small test pulse to -40 mV, but became outward after stronger test pulses. This behavior indicated that without DTT treatment the S631C channels might exist as a mixed population of "WT-like" and mutant forms. In the experiment shown in Fig. 10, repetitive depolarization pulses to $+40$ mV for 1 s each caused a gradual change in the channel properties. At the steady state of these changes (after 28 pulses), the current appeared to be in purely mutant form. Test pulse currents increased in the inward direction during depolarization steps to V_t from -60 to -30 mV, but increased in the outward direction during stronger depolarization steps. There was no sign of inward rectification up to $+60$ mV. These were followed by inward tail currents at -80 mV. Similar observations were obtained in 10 experiments, although the rate and degree of phenotype switch induced by 1-s depolarization pulses to $+40$ mV varied among oocytes. After a switch in the phenotype, DTT caused a rapid reversal (Fig. 10, *right panel*). These observations suggest that membrane depolarization induced a rearrangement of outer mouth residues that brought the thiol groups at position 631 from different subunits close to each other, facilitating disulfide bond formation between them. This was associated with a phenotype switch similar to that induced by H_2O_2 or MTS reagents.

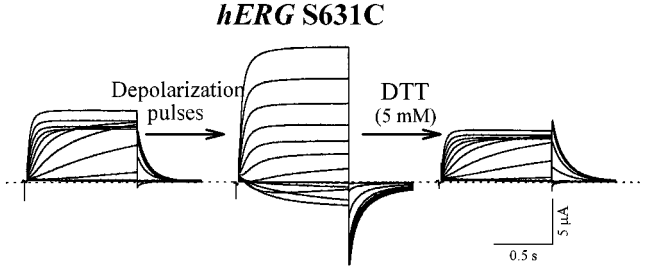

FIGURE 10 Switch of *hERG* S631C channel phenotype induced by repetitive depolarization pulses (28 pulses to $+40$ mV for 1 s each) and its reversal by a thiol-reducing agent (5 mM DTT).

DISCUSSION

Comparison with previous studies on *hERG*

The effects of S631 mutations on C-type inactivation of *hERG* have been described in several reports before (Schonherr and Heinemann, 1996; Smith et al., 1996; Herzberg et al., 1998; Zou et al., 1998). Our observations that C-type inactivation was attenuated in S631A and abolished in S631V are similar to those of others. The new results presented here are from other mutations (S631Y, S631K, S631E, and, in particular, S631C). Furthermore, we examined how these mutations could affect channel functions in addition to C-type inactivation.

The major findings of this study can be summarized as follows. The behavior of S631 mutants can be segregated into two types. Mutations that retained C-type inactivation (S631Y and S631A) maintained a high K selectivity and the same voltage dependence of activation as the WT channel. Mutations that disrupted C-type inactivation (S631V, S631K, and S631E) also reduced the channels' K selectivity (conducting Na ions in the presence of K) and altered the voltage dependence of activation (causing a hyperpolarizing shift in $V_{0.5}$ of activation, along with an appearance of a shallow component of channel activation in the positive voltage range). A more direct linkage between 631 side-chain properties and channel functions was seen in the S631C mutant. S631C channels that had thiol groups in the reduced state (free thiol groups) behaved like the WT channel. S631C channels with thiol groups modified by an oxidizing agent (H_2O_2) or by MTSET or MTSES displayed a mutant behavior similar to that described above for S631V, S631K, and S631E. These thiol modifying reagents did not affect the properties of the WT channel.

The correlation between the loss of C-type inactivation and the loss of K selectivity in some of the S631 mutant channels is consistent with the notion that these two processes are intimately related physically and functionally (Kiss and Korn, 1998; Kiss et al., 1999; Starkus et al., 1997). For example, it has been shown that the onset of C-type inactivation of Kv2.1 is preceded by a reduction in the pore's K selectivity (Kiss et al., 1999). However, this tight linkage raises a concern: is it possible that the lack of C-type inactivation in these mutants was due to Na ions binding within the pore that hindered C-type inactivation, similar to the effects elevating $[K]_o$ on the WT *hERG* channel (Wang et al., 1996; Sanguinetti et al., 1995)? This is not likely, because a total removal of extracellular Na ions did not restore C-type inactivation in S631V, S631K, S631E, or S631C (H_2O_2-treated) (Figs. 5 and 8).

Comparison with equivalent mutations of T449 in the Shaker channel

When comparing the effects of S631 mutations with those of T449 mutations in the *Shaker* channel, only S631V showed an effect similar to that of T449V: C-type inactivation was abolished in both (Ogielska et al., 1995; Lopez-Barneo et al., 1993). The others were either different (S631Y retained C-type inactivation in *hERG*, whereas T449Y abolishes C-type in *Shaker*), or opposite (S631K and S631E disrupted C-type inactivation in *hERG*, whereas T449K and T449E greatly facilitated C-type inactivation in *Shaker*; S631A retained C-type inactivation but to a lesser degree than that of WT *hERG*, whereas T449A enhanced C-type inactivation in *Shaker*) (Ogielska et al., 1995; Lopez-Barneo et al., 1993). These data suggest that although C-type inactivation involves residues in the outer mouth region in both *hERG* and *Shaker*, different structural determinants are involved. Furthermore, the loss of K selectivity accompanying the loss of C-type inactivation seen in S631K and S631E of *hERG* is not seen in T449K or T449E of *Shaker*, again pointing to differences in the outer mouth structure between these two channels (Molina et al., 1997; Ogielska et al., 1995; Lopez-Barneo et al., 1993).

Implications for differences in the outer mouth structure between *hERG* and *Shaker*

Two observations suggest that the outer mouth of *hERG* around position 631 is probably narrower than that of *Shaker* around position 449. First, S631C of *hERG* could form disulfide bonds spontaneously (Fig. 10), whereas T449C of *Shaker* cannot (Liu et al., 1996). However, M448C, which is one residue deeper into the pore and thus is in a more confined environment, can form disulfide bonds with other M448C across subunits (Liu et al., 1996). Second, the S631Y mutation did not enhance the channel's sensitivity to extracellular TEA (data not shown), suggesting that this extracellular blocker cannot reach the side chain at position 631. This is in sharp contrast to the situation in the *Shaker* channel: T449Y greatly increases the channel's sensitivity to external TEA by allowing interactions between the blocker's positive charge and π electrons of tyrosine residues in the outer mouth region (Heginbotham and MacKinnon, 1992).

The crystal structure of a K channel pore (KcsA) and its surrounding transmembrane α-helices is available (Doyle et al., 1998). These data suggest that interactions between aromatic residues at the two ends of the P-loop sequence are an important determinant for the outer mouth dimension. This may provide a clue to why the outer mouth dimension may differ between *hERG* and *Shaker* channels. According to the crystal structure data, the two tryptophan residues (WW) at the amino end and the tyrosine (Y) at the carboxy end of the P-loop sequence form a massive aromatic sheet that is like a cuff around the outer mouth region of the pore (Doyle et al., 1998). This sheet of aromatic interactions serves the function of a "molecular spring" that pulls the outer mouth in the radial direction, keeping the outer pore open to a certain width, so that the channel can select for dehydrated K ions better than for dehydrated Na ions. The interactions include hydrogen bonds between the nitrogens of the tryptophan residues and the hydroxyl group of the tyrosine residue, as well as van der Waals forces between these aromatic structures (Doyle et al., 1998). The *Shaker* P-loop sequence has both tryptophan residues at the amino end and the tyrosine at the carboxy end (Fig. 1). The importance of hydrogen bonds between tryptophan and tyrosine residues in the function of this "molecular spring" is supported by the observations that if one of the tryptophans is mutated to phenylalanine (W434F) (Yang et al., 1997) or if the tyrosine is mutated to valine (F445V) (Heginbotham et al., 1994), so that the hydrogen bonds are interrupted, the channel tends to be persistently C-type inactivated, as if removing the hydrogen bonds and weak-

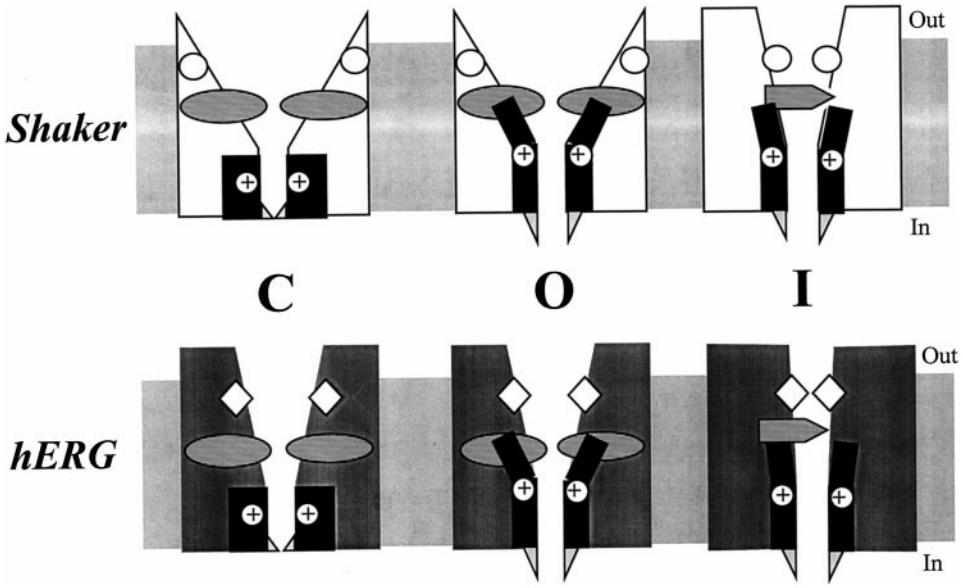

FIGURE 11 Hypothesis for why equivalent mutations can cause different effects on C-type inactivation between *Shaker* and *hERG*. For both channels the pore is depicted as an "inverted teepee" through the membrane (Doyle et al., 1998), with the following features: 1) voltage sensor (*black area shown with a positive sign*) and activation gate (*stippled triangles*) that control the opening and closing of the cytoplasmic entrance to the pore (Holmgren et al., 1998; Shieh et al., 1997; Larsson et al., 1996); 2) ion selectivity filter and C-type inactivation gate that are close to each other (shown as *striped symbols*) (Kiss and Korn, 1998) and to the extracellular entrance to the pore, the conformation of which depends on the gating state of the channel: C (closed or rested state), O (open state), and I (C-type inactivated state) (Doyle et al., 1998; Liu et al., 1996); and 3) position 449 (*open circles* in *Shaker*) or 631 (*open diamonds* in *hERG*) that are equivalent to each other and are located in the outer mouth region of the pores.

ening the strength of the molecular spring make the outer mouth constrict more easily.

In the *hERG*'s P-loop sequence, the tryptophan residues at the amino end are replaced by tyrosine and phenylalanine (YF), and the tyrosine at the carboxy end is replaced by phenylalanine (F) (Fig. 1). Therefore, no hydrogen bonds are possible between these aromatic residues. This may weaken the molecular spring and cause *hERG*'s outer mouth to be narrower than the *Shaker* channel. This is depicted in Fig. 11.

According to this hypothesis (Fig. 11), the *Shaker* channel has a wider outer mouth because of a strong molecular spring around the outer mouth. C-type inactivation can bring residues at position 449 from different subunits closer to each other. However, these residues still have sufficient distance between them such that when cysteine residues occupy this position (T449C) they cannot form disulfide bonds with each other. When glutamate or lysine residues occupy this position (T449E or T449K), there is no repulsion between the like charges from different subunits. On the other hand, these charged residues stabilize the channel in the C-type inactivated state because of their hydrophilic nature.

Fig. 11 depicts a narrower outer mouth in the *hERG* channel due to a weaker molecular spring around this region. As a result, C-type inactivation will bring the residues at position 631 from different subunits much closer to each other than is the case for position 449 in the *Shaker* channel. When cysteine residues occupy position 631 in the four subunits (S631C), membrane depolarization and thus C-type inactivation will bring them close enough to each other to form disulfide bonds. When this occurs, the rigidity of disulfide bonds in the outer mouth region hinders the dynamic rearrangements needed for the C-type inactivation process. This also reduces the channel's K selectivity, because K ion selection and permeation through the pore is a dynamic process, involving movements of side chains and the peptide backbone around the selectivity filter (Durell and Guy, 1996; Heginbotham et al., 1994). Furthermore, when glutamate or lysine residues occupy this position in the four subunits (S641E or S631K), the repulsion between like charges will limit the degree of freedom of side chain and backbone movements, leading to a disruption of C-type inactivation and K selectivity.

The strength of the "molecular spring" may affect the efficiency of coupling between S4 movements and changes in the outer mouth conformation. The stronger molecular spring in the Shaker channel makes the outer mouth more resistant to the forces that tend to constrict the pore. The weaker molecular spring in the *hERG* channel makes the outer mouth conform to the forces more readily. This hypothesis must be tested by mutating *hERG*'s P-loop sequence to confer the ability of hydrogen bond formation between aromatic residues around the outer mouth region, and by observing how these and further S631 mutations can affect the rate of C-type inactivation.

This work was supported by HL 46451 (to G-NT) from the National Heart, Lung and Blood Institute, National Institutes of Health, Bethesda, MD.

REFERENCES

Baukrowitz, T., and G. Yellen. 1995. Modulation of K^+ current by frequency and external [K^+]: a tail of two inactivation mechanisms. *Neuron.* 15:951–960.

Cha, A., and F. Bezanilla. 1998. Structural implications of fluorescence quenching in the *Shaker* K^+ channel. *J. Gen. Physiol.* 112:391–408.

Choi, K. L., R. W. Aldrich, and G. Yellen. 1991. Tetraethylammonium blockade distinguishes two inactivation mechanisms in voltage-activated K^+ channels. *Proc. Natl. Acad. Sci. USA.* 88:5092–5095.

Doyle, D. A., J. M. Cabral, R. A. Pfuetzner, A. Kuo, J. M. Gulbis, S. L. Cohen, B. T. Chait, and R. MacKinnon. 1998. The structure of the potassium channel: molecular basis of K^+ conduction and selectivity. *Science.* 280:69–77.

Durell, S. R., and H. R. Guy. 1996. Structural model of the outer vestibule and selectivity filter of the *Shaker* voltage-gated K^+ channel. *Neuropharmacology.* 35:761–773.

Ficker, E., W. Jarolimek, J. Kiehn, A. Baumann, and A. M. Brown. 1998. Molecular determinants of dofetilide block of HERG K^+ channels. *Circ. Res.* 82:386–395.

Hancox, J. C., A. J. Levi, and H. J. Witchel. 1998. Time course and voltage dependence of expressed HERG current compared with native "rapid" delayed rectifier K current during the cardiac ventricular action potential. *Pflugers Arch.* 436:843–853.

Heginbotham, L., Z. Lu, T. Abramson, and R. MacKinnon. 1994. Mutations in the K^+ channel signature sequence. *Biophys. J.* 66:1061–1067.

Heginbotham, L., and R. MacKinnon. 1992. The aromatic binding site for tetraethylammonium ion on potassium channels. *Neuron.* 8:483–491.

Herzberg, I. M., M. C. Trudeau, and G. A. Robertson. 1998. Transfer of rapid inactivation and sensitivity to the class III antiarrhythmic drug E-4031 from HERG to M-eag channels. *J. Physiol. (Lond.).* 511:3–14.

Hille, B. 1992. Selective permeability: independence. *In* Ionic Channels of Excitable Membranes, 2nd Ed. B. Hille, editor. Sinauer Associates, Sunderland, MA. 337–361.

Holmgren, M., K. S. Shin, and G. Yellen. 1998. The activation gate of a voltage-gated K^+ channel can be trapped in the open state by an intersubunit metal bridge. *Neuron.* 21:617–621.

Hoshi, T., W. N. Zagotta, and R. W. Aldrich. 1991. Two types of inactivation on Shaker K^+ channels: effects of alterations in the carboxy-terminal region. *Neuron.* 7:547–556.

Kiss, L., D. Immke, J. LoTurco, and S. J. Korn. 1998. The interaction of Na^+ and K^+ in voltage-gated potassium channels. Evidence for cation binding sites of different affinity. *J. Gen. Physiol.* 111:195–206.

Kiss, L., and S. J. Korn. 1998. Modulation of C-type inactivation by K^+ at the potassium channel selectivity filter. *Biophys. J.* 74:1840–1849.

Kiss, L., J. LoTurco, and S. J. Korn. 1999. Contribution of the selectivity filter to inactivation in potassium channels. *Biophys. J.* 76:253–263.

Larsson, H. P., O. S. Baker, D. S. Dhillon, and E. Y. Isacoff. 1996. Transmembrane movement of the shaker K^+ channel S4. *Neuron.* 16: 387–397.

Liu, Y., M. E. Jurman, and G. Yellen. 1996. Dynamic rearrangement of the outer mouth of a K^+ channel during gating. *Neuron.* 16:859–867.

Loots, E., and E. Y. Isacoff. 1998. Protein rearrangements underlying slow inactivation of the *Shaker* K^+ channel. *J. Gen. Physiol.* 112:377–389.

Lopez-Barneo, J., T. Hoshi, S. H. Heinemann, and R. W. Aldrich. 1993. Effects of external cations and mutations in the pore region on C-type inactivation of Shaker potassium channels. *Receptors Channels.* 1:61–71.

Molina, A., A. G. Castellano, and J. Lopez-Barneo. 1997. Pore mutations in *Shaker* K^+ channels distinguish between the sites of tetraethylammonium blockade and C-type inactivation. *J. Physiol. (Lond.).* 499: 361–367.

Ogielska, E. M., W. N. Zagotta, T. Hoshi, S. H. Heinemann, J. Haab, and R. W. Aldrich. 1995. Cooperative subunit interactions in C-type inactivation of K channels. *Biophys. J.* 69:2449–2457.

Panyi, G., Z.-F. Sheng, L.-W. Tu, and C. Deutsch. 1995. C-type inactivation of a voltage-gated K^+ channel occurs by a cooperative mechanism. *Biophys. J.* 69:896–903.

Rasmusson, R. L., M. J. Morales, S. Wang, S. Liu, D. L. Campbell, M. V. Brahmajothi, and H. C. Strauss. 1998. Inactivation of voltage-gated cardiac K^+ channels. *Circ. Res.* 82:739–750.

Roden, D. M., R. Lazzara, M. R. Rosen, P. J. Schwartz, J. Towbin, and G. M. Vincent. 1996. Multiple mechanisms in the long-QT syndrome. Current knowledge, gaps, and future directions. *Circulation.* 94: 1996–2012.

Sanguinetti, M. C., C. Jiang, M. E. Curran, and M. T. Keating. 1995. A mechanistic link between an inherited and an acquired cardiac arrhythmia: HERG encodes the I_{Kr} potassium channel. *Cell.* 81: 299–307.

Schonherr, R., and S. H. Heinemann. 1996. Molecular determinants for activation and inactivation of HERG, a human inward rectifier potassium channel. *J. Physiol. (Lond.).* 493:635–642.

Schreibmayer, W., H. A. Lester, and N. Dascal 1994. Voltage clamping of *Xenopus laevis* oocytes utilizing agarose-cushion electrodes. *Pflugers Arch.* 426:453–458.

Shieh, C.-C., K. G. Klemic, and G. E. Kirsch. 1997. Role of transmembrane segment S5 on gating of voltage-dependent K^+ channels. *J. Gen. Physiol.* 109:767–778.

Shigeru, O. 1989. Oxidation and oxygenation. *In* Organic Sulfur Chemistry: Structure and Mechanism. D. J. Takahashi, editor. CRC Press, Boston. 203–291.

Smith, P. A., T. Baukrowitz, and G. Yellen. 1996. The inward rectification mechanism of the HERG cardiac potassium channel. *Nature.* 379: 833–836.

Spector, P. S., M. E. Curran, A. Zou, M. T. Keating, and M. C. Sanguinetti. 1996. Fast inactivation causes rectification of the I_{Kr} channel. *J. Gen. Physiol.* 107:611–619.

Starkus, J. G., L. Kuschel, M. D. Rayner, and S. H. Heinemann. 1997. Ion conduction through C-type inactivated *Shaker* channels. *J. Gen. Physiol.* 110:539–550.

Trudeau, M. C., J. W. Warmke, B. Ganetzky, and G. A. Robertson. 1995. HERG, a human inward rectifier in the voltage-gated potassium channel family. *Science.* 269:92–95.

Wang, S., S. Liu, M. J. Morales, H. C. Strauss, and R. L. Rasmusson. 1997. A quantitative analysis of the activation and inactivation kinetics of *HERG* expressed in *Xenopus* oocytes. *J. Physiol. (Lond.).* 502:45–60.

Wang, S., M. J. Morales, S. Liu, H. C. Strauss, and R. L. Rasmusson. 1996. Time, voltage and ionic concentration dependence of rectification of h-erg expressed in *Xenopus* oocytes. *FEBS Lett.* 389:167–173.

Yang, Y., Y.-Y. Yang, and F. J. Sigworth. 1997. How does the W434F mutation block current in *Shaker* potassium channels? *J. Gen. Physiol.* 109:779–789.

Yellen, G., D. Sodickson, T.-Y. Chen, and M. E. Jurman. 1994. An engineered cysteine in the external mouth of a K^+ channel allows inactivation to be modulated by metal binding. *Biophys. J.* 66: 1068–1075.

Zhou, J., Q. Gong, B. Ye, Z. Fan, J. C. Makielski, G. A. Robertson, and C. T. January. 1998. Properties of HERG channels stably expressed in HEK 293 cells studied at physiological temperature. *Biophys. J.* 74: 230–241.

Zou, A., Q. P. Xu, and M. C. Sanguinetti. 1998. A mutation in the pore region of HERG K^+ channels expressed in *Xenopus* oocytes reduces rectification by shifting the voltage dependence of inactivation. *J. Physiol. (Lond.).* 509:129–137.